



OPEN ACCESS

EDITED BY

Yilei Zhang,
Department of Biochemistry and
Molecular Biology, Xi'an Jiaotong
University, China

REVIEWED BY

Zhen Shu,
Emory University, United States
Zhuoyu Gu,
Fifth Affiliated Hospital of Zhengzhou
University, China

*CORRESPONDENCE

Haifeng Zhang,
✉ zhf19841011@126.com
Lihong Fan,
✉ lhfan@xjtu.edu.cn

[†]These authors have contributed equally
to this work

RECEIVED 30 March 2023

ACCEPTED 09 May 2023

PUBLISHED 23 May 2023

CITATION

Jing Z, Zhang H, Wen Y, Cui S, Ren Y,
Liu R, Duan S, Zhao W and Fan L (2023),
Epigenetic and transcriptomic alterations
in the CIC-3-deficient mice consuming a
normal diet.
Front. Cell Dev. Biol. 11:1196684.
doi: 10.3389/fcell.2023.1196684

COPYRIGHT

© 2023 Jing, Zhang, Wen, Cui, Ren, Liu,
Duan, Zhao and Fan. This is an open-
access article distributed under the terms
of the [Creative Commons Attribution
License \(CC BY\)](https://creativecommons.org/licenses/by/4.0/). The use, distribution or
reproduction in other forums is
permitted, provided the original author(s)
and the copyright owner(s) are credited
and that the original publication in this
journal is cited, in accordance with
accepted academic practice. No use,
distribution or reproduction is permitted
which does not comply with these terms.

Epigenetic and transcriptomic alterations in the CIC-3-deficient mice consuming a normal diet

Zhenghui Jing^{1,2†}, Haifeng Zhang^{1,2*†}, Yunjie Wen^{3†}, Shiyu Cui^{1,2},
Yuhua Ren^{1,2}, Rong Liu^{1,2}, Sirui Duan⁴, Wenbao Zhao¹ and
Lihong Fan^{4*}

¹Department of Pathology of Basic Medicine College, Xi'an Jiaotong University, Xi'an, China, ²Institute of Genetics and Developmental Biology of Translational Medicine Institute, Xi'an Jiaotong University, Xi'an, Shaanxi, China, ³Guangzhou Huayin Medical Laboratory Center Ltd., Guangzhou, Guangdong, China, ⁴Department of Cardiovascular Medicine, The First Affiliated Hospital of Xi'an Jiaotong University, Xi'an, Shaanxi, China

Introduction: Metabolic disorders are an important health concern that threatens life and burdens society severely. CIC-3 is a member of the chloride voltage-gated channel family, and CIC-3 deletion improved the phenotypes of dysglycemic metabolism and the impairment of insulin sensitivity. However, the effects of a healthy diet on transcriptome and epigenetics in CIC-3^{-/-} mice were not explained in detail.

Methods: Here, we performed transcriptome sequencing and Reduced Representation Bisulfite Sequencing for the liver of 3 weeks old WT and CIC-3^{-/-} mice consuming a normal diet to insight into the epigenetic and transcriptomic alterations of CIC-3 deficient mice.

Results: In the present study, we found that CIC-3^{-/-} mice that were younger than 8 weeks old had smaller bodies compared to CIC-3^{+/+} mice with ad libitum self-feeding normal diet, and CIC-3^{-/-} mice that were older than 10 weeks old had a similar body weight. Except for the spleen, lung, and kidney, the average weight of the heart, liver, and brain in CIC-3^{-/-} mice was lower than that in CIC-3^{+/+} mice. TG, TC, HDL, and LDL in fasting CIC-3^{-/-} mice were not significantly different from those in CIC-3^{+/+} mice. Fasting blood glucose in CIC-3^{-/-} mice was lower than that in CIC-3^{+/+} mice; the glucose tolerance test indicated the response to blood glucose increasing for CIC-3^{-/-} mice was torpid, but the efficiency of lowering blood glucose was much higher once started. Transcriptomic sequencing and reduced representation bisulfite sequencing for the liver of unweaned mice indicated that CIC-3 deletion significantly changed transcriptional expression and DNA methylation levels of glucose metabolism-related genes. A total of 92 genes were intersected between DEGs and DMRs-targeted genes, of which *Nos3*, *Pik3r1*, *Socs1*, and *Acly* were gathered in type II diabetes mellitus, insulin resistance, and metabolic pathways. Moreover, *Pik3r1* and *Acly* expressions were obviously correlated with DNA methylation levels, not *Nos3* and *Socs1*. However, the transcriptional levels of these four genes were not different between CIC-3^{-/-} and CIC-3^{+/+} mice at the age of 12 weeks.

Discussion: CIC-3 influenced the methylated modification to regulate glucose metabolism, of which the gene expressions could be driven to change again by a personalized diet-style intervention.

KEYWORDS

glucose metabolism, CIC-3, genetically modified mice, DNA methylation, normal diet

1 Introduction

The prevalence of metabolic disorders is steadily rising along with the improvement of living quality. According to the International Diabetes Federation (IDF) Diabetes Atlas, it is estimated that 537 million people have diabetes and 541 million people are suffering from impaired glucose tolerance in 2021 (Sun et al., 2022). The metabolic dysfunction of glucose has been one of the non-negligible risks, threatening human life and curbing social and economic development. Thus, it is urgent to identify efficient molecular targets to rebalance the dysfunction of glucose metabolism.

Epigenetics is a heritable and reversible modification that acts as a mediator of gene–environmental interactions. DNA methylation, an essential epigenetic modification to silence gene expression, has been focused on as a clinical biomarker in cancer (Jin et al., 2009; Payne, 2010), aging (Teschendorff et al., 2010), obesity (Xu et al., 2013; Aslibekyan et al., 2015), cardiovascular events (Hu et al., 2021; Qin et al., 2021), Alzheimer's disease (Shao et al., 2018), etc. Gathered evidence demonstrated that aberrant DNA methylation was closely related to diabetes. For instance, pancreatic duodenal homeobox 1 (PDX-1) mutations can cause a monogenic form of maturity-onset diabetes of the young, in which the CpG sites in the distal promoter and enhancer regions exhibited significantly increased DNA methylation in the pancreatic islets of type 2 diabetes (T2D) patients (Yang et al., 2012). Furthermore, the genome-wide survey revealed predisposing T2D-related DNA methylation variations in human peripheral blood, including *CENTD2*, *FTO*, *KCNJ11*, *TCF7L2*, and *WFS1* (Toperoff et al., 2012).

ClC-3 chloride channels are widely expressed in most mammalian cells and are primarily localized on cell and organelle membranes. Regarding the important roles in the vasculature's pathological changes, ClC-3 was considered a promising therapeutic target for cardiovascular diseases (CVDs) (Duan, 2011; Du and Guan, 2015; Niu et al., 2021). It is well known that diabetes, dyslipidemia, and hypertension are CVDs' most common risk factors. ClC-3 could mediate the processing and release of insulin through the regulation of granular acidification (Deriy et al., 2009; Li et al., 2009). ClC-3 deficiency attenuated hyperglycemia, hyperlipidemia, and insulin resistance in type 2 diabetes mellitus (Huang et al., 2014), and it ameliorated high-fat diet-induced obesity, which promoted the development of glucose and lipid metabolism disorders (Ma et al., 2019). It is supposed that ClC-3 would be a potential target to improve the dysfunction of glucose or lipid metabolism.

ClC-3 silencing remarkably refined glucose and lipid metabolism in animals intaking an abnormal diet, but the underlying mechanisms were not clearly elucidated, especially the changes of metabolism-related gene modification. The existence of a gene is the foundation of its expression, but the expression levels are the results of a life entity responding to the environment. Thus, this study primarily demonstrated the influence of a normal diet on transcriptome and DNA methylation in ClC-3 knockout mice.

2 Materials and methods

2.1 Animals

ClC-3 knockout mice were obtained from the mating of heterozygous mice, which were produced via the CRISPR-cas9 technique (Cyagen, China) and gifted by Doctor Deng from the First Affiliated Hospital of Shen Zhen University. The mice were fed under a 12-h dark/light cycle with *ad libitum* self-feeding in specific pathogen-free conditions of 55% humidity and 22°C. All animal experimental procedures were approved by the Laboratory Animal Administration Committee of Xi'an Jiaotong University (2021-1499).

The wild-type (ClC-3^{+/+}), heterozygous (ClC-3^{+/-}), and homozygous mice (ClC-3^{-/-}) were identified by a polymerase chain reaction following our previous work (Jing et al., 2022). The length of the PCR product for the WT ClC-3 was 769 bp, for which the sequences of primers were TTAGTGCTGGCTGTGGCATC (F1) and TCCCAGAGACAA TGAGGCTAAGG (R). The PCR product of 654 bp was for the mutated ClC-3, and the sequences of primers were TCTGAT GGGGACTAAGTATGCAG (F2) and TCCCAGAGACAA TGAGGCTAAGG (R).

2.2 Serum and tissue sample collection

The unweaned mice at the age of 3 weeks were anesthetized with 0.03% pentobarbital sodium solution and then euthanized by cervical dislocation; their liver, kidney, lung, heart, spleen, and brain were dissected, photographed, and stored at -80°C. The 4-week-old ClC-3^{+/+} and ClC-3^{-/-} mice were fed a normal diet and weighed weekly. After 8 weeks, all mice were anesthetized with 0.03% pentobarbital sodium solution; the blood obtained from the heart was placed at 4°C for 2 h and then centrifuged at 4,000 rpm for 15 min to harvest serum; the principal parenchymal organs of 12-week-old mice were then dissected, weighed, photographed, and cryopreserved.

2.3 Glucose tolerance and blood lipid test

The 12-week-old adult mice were rolled into the glucose tolerance test. After being made to fast for 12 h, the mice were intraperitoneally injected with D-glucose doses of 2 g per kilogram body weight (CAS-50997, Sigma-Aldrich, United States); the glucose of tail blood at 0, 15, 30, 60, 90, and 120 min after injection was measured using a glucometer (Accu-Chek-Guide, Roche, Germany), respectively. The time–concentration curves of blood glucose for ClC-3^{+/+} and ClC-3^{-/-} mice were plotted and standardized according to the fasting blood glucose.

After the 12-week-old mice fasted overnight, the total cholesterol (TC), triglyceride (TG), high-density lipoprotein (HDL), and low-density lipoprotein (LDL) were assayed with an automated biochemical analyzer (BS-800, Mindray, China).

TABLE 1 Primer sequences for qPCR used in the study.

Gene	Forward primer	Reverse primer
GAPDH	CAGTGGCAAAGTGGAGATTGTTG	TCGCTCCTGGAAGATGGTGAT
Nos3	GGTTGCAAGGCTGCCAATTT	TAACTACCACAGCCGGAGGA
Pik3r1	CTATGCCTGCTCCGTAGTGG	TCATCGCCTCTGTGTGCAT
AclY	GTTGCGTTGTGGACATGCT	ATCCCAGGGGTGACGATACA
Socs1	CGAGACCTTCGACTGCCTTT	AGTCACGGAGTACCGGGTTA

2.4 Transcriptomics

The transcriptome of a 3-week-old mouse's liver was sequenced by the Huayin Health Medical Group Company (Guangzhou, China). In brief, total RNAs were extracted using the TRIzol reagent (cat.265709, Life, United States) following the manufacturer's instructions. After being qualified and quantified by the Agilent 2100 Bioanalyzer (Agilent, United States) and NanoPhotometer[®] (Implen, Germany), 1 µg RNA was used to purify mRNA via the VAHTS[®] mRNA Capture Beads with Oligo dT (cat.N401-01, Vazyme Biotech, China). Subsequently, mRNA was reversely transcribed into the double-strand cDNA with VAHTS[®] Universal V6 RNA-seq Library Prep Kit (cat.NR604, Vazyme Biotech, China). Then, cDNA was added to an A base and digested with the UDG enzyme. Favorable cDNA fragments were selected for PCR amplification to establish the cDNA library. Finally, 2 × 150 bp paired-end sequencing was performed on a NovaSeq[™] 6000 system (Illumina Corporation, United States) under the vendor's guidance.

Raw reads proceeded to quality control, and then, clean data were obtained. After being blasted with the mouse reference genome (mmu10), the algorithm of RNASeq by Expectation Maximization (RSEM) was adopted to compute the gene expressions, of which the differential expression analysis between *C1C-3^{+/+}* and *C1C-3^{-/-}* mice was done with edgeR (Robinson, United States). The genes with $|\log_2\text{Ratio}| \geq 1$ and $p\text{-value} < 0.05$ were regarded as differentially expressed genes (DEGs), which were furtherly explored by the enrichment of Kyoto Encyclopedia of Genes and Genomes (KEGG) pathways.

2.5 Quantitative real-time polymerase chain reaction

The total RNA of livers in 12-week-old mice was extracted by TRIzol reagent (#R4801, Magen, China) according to the instruction and quantified with a nanodrop instrument (DeNovix, United States). A total of 1 µg RNA was reverse-transcribed into complementary DNA (cDNA) using a reverse transcription kit (#1137ES60, Yeasen, China). The qPCR was performed using a CFX real-time system (Bio-Rad, United States), and the machine parameters were pre-degeneration at 95°C for 5 min; denaturation at 95°C for 10 s, and annealing and extension at 60°C for 30 s for 40 cycles were performed. The 2^{-ΔΔCT} method was used to calculate the relative expression of genes. GAPDH was used as a reference

gene for analyzing target gene expression. The primer sequences used in the study are listed in Table 1.

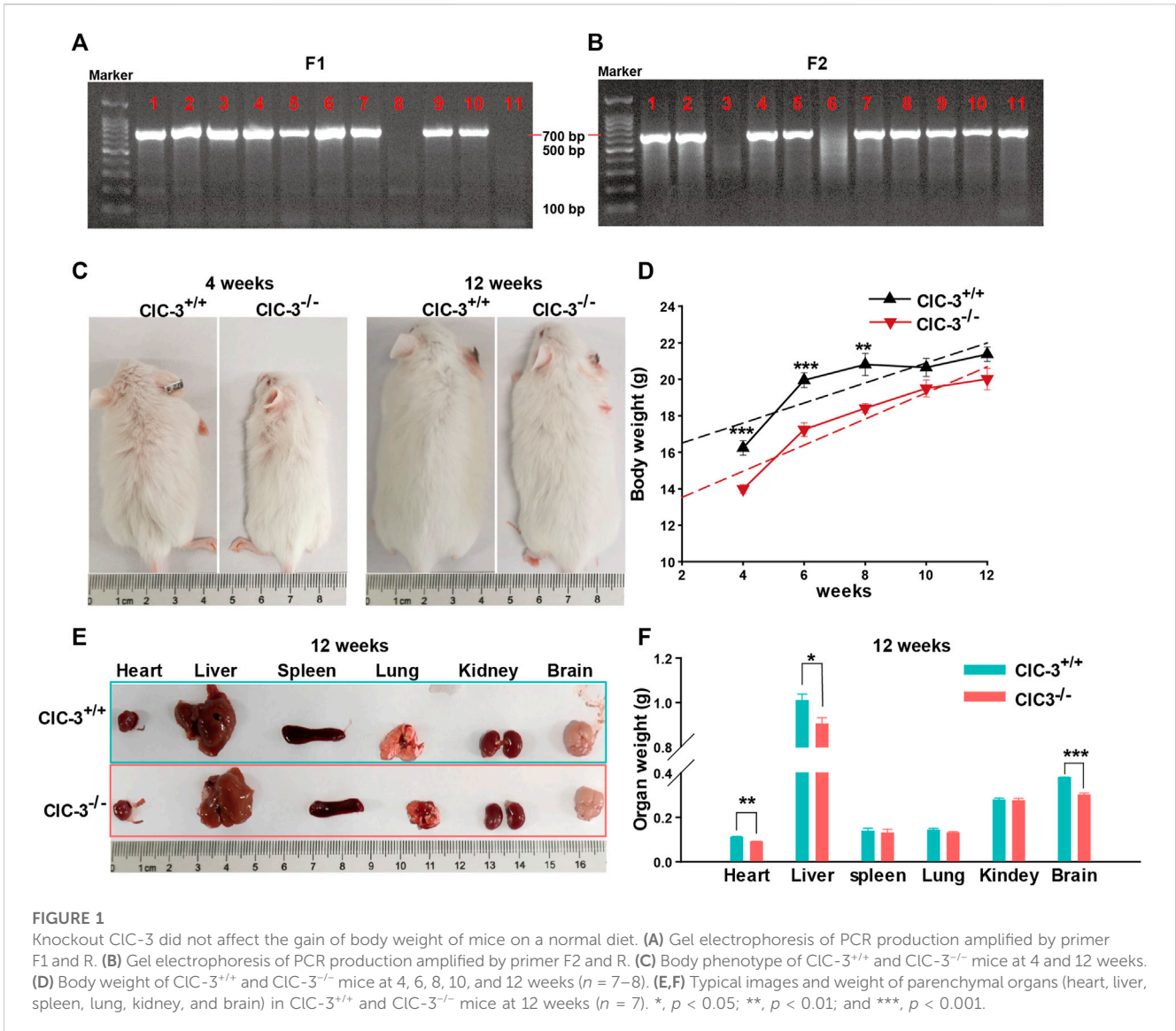
2.6 Reduced representation bisulfite sequencing

Reduced representation bisulfite sequencing (RRBS) was performed to analyze the DNA methylations of liver tissues, which were the same samples being used in transcriptome sequencing. In brief, the genomic DNA was isolated with the QIAamp[®] Blood and Tissue Kit (cat.51104, Qiagen, Germany). After the quality inspection of DNA, 100 ng DNA was digested with MspI, end-repaired, 3'-dA-tailed, and ligated to 5-methylcytosine-modified adapters. DNAs were treated with bisulfite and then amplified via PCR to establish RRBS libraries, of which the concentration and fragment size were detected by using Agilent 2100 Bioanalyzer and Qubit assay tubes (cat.1604220, Life, United States). Finally, 2 × 150 bp paired-end sequencing was performed on an Illumina NovaSeq[™] 6000 system following the vendor's recommended protocol.

The low-quality reads and sequencing adapters were trimmed from the sequencing raw data to obtain clean data using Trimmomatic software (version 0.40, Germany). DNA methylation information was obtained by blasting clean data with the mouse reference genome (mmu10) using the BSMAP protocol (version 2.90). The differentially methylated regions (DMRs) in the CG context were analyzed with a binary segmentation algorithm combined with the MWU-test and 2D KS-test using metilene software (version 0.2.8, United States). DMR-targeted genes were enriched by the analysis of KEGG pathways.

2.7 Conjoint analysis of transcriptomics and DNA methylation

The sample used in methylation sequencing was incised from the corresponding liver tissue in transcriptome sequencing, so the conjoint analysis of these data could be executed. After the DEGs in transcriptomics and DMR-targeted genes were intersected, the mutual genes were analyzed with the enrichment of KEGG pathways. Moreover, the Pearson correlations between the intersected gene expressions and their DNA methylation levels were computed.



2.8 Statistical analysis

All data were presented as mean ± standard error. The difference between the two groups was tested by an independent Student’s *t*-test, and a *p*-value less than 0.05 was considered significantly different. All statistical analyses were performed with SigmaPlot software (v12.5, Systat Software Inc., United States).

3 Results

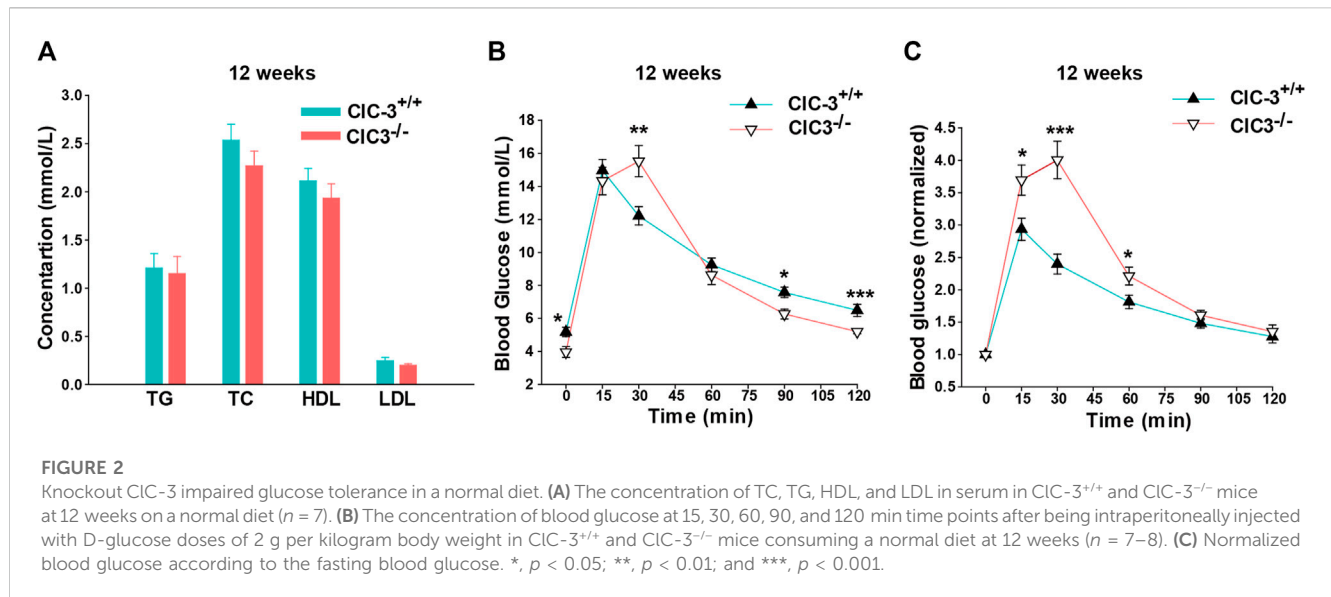
3.1 The deletion of CIC-3 did not impede the weight gain of CIC-3^{-/-} mouse consuming a normal diet

CIC-3^{-/-} mice with breast milk or high-fat diets gained lower body weight (Jing et al., 2022), indicating the important roles of CIC-3 in energy metabolism. The manifestations were the results of the interactions between the genes and environment, including

diet, lifestyle, and emotion. However, there is no idea about the effects of *ad libitum* self-feeding normal diet on the growth of CIC-3^{-/-} mice.

As shown in Figures 1A, B, DNA was extracted from the tail of 3-week-old mice and amplified by PCR to determine the CIC-3 genotype; there was only one band of 769 bp PCR product for CIC-3^{+/+} mice and one 654 bp band for CIC-3^{-/-} mice, and two bands indicated the heterozygous mice. Compared to 4-week-old CIC-3^{+/+} mice, CIC-3^{-/-} mice were obviously smaller; their average body weight was 13.99 ± 0.24 g. Mice were fed with a normal diet and grown to 10 weeks old, and the average body weights for CIC-3^{+/+} and CIC-3^{-/-} mice were 20.65 ± 0.5 and 19.5 ± 0.47 g, respectively (n = 7–8, *p* > 0.05). There was no difference in body weight between CIC-3^{+/+} and CIC-3^{-/-} mice at the 12 weeks (n = 7–8, *p* > 0.05, Figures 1C, D). It is suggested that the growth of mice consuming a normal diet was not obviously slowed by the CIC-3 gene deletion.

Moreover, the major parenchymal organs in 12-week-old mice were dissected, photographed, and weighed. As illustrated in Figures 1E, F, there were no differences in the spleen, lung,



and kidney weights for CIC-3^{+/+} and CIC-3^{-/-} mice ($n = 7$, $p > 0.05$), which were not consistent with those observed in the unweaned mice (Jing et al., 2022). The average weight of the heart, liver, or brain in CIC-3^{-/-} mice was lower than that in CIC-3^{+/+} mice ($n = 7$, $p < 0.05$); the total weights of the heart, liver, and brain in CIC-3^{+/+} and CIC-3^{-/-} mice only accounted for $7.07\% \pm 0.17\%$ and $6.58\% \pm 0.16\%$ of the whole body weights, respectively ($n = 7$, $p > 0.05$). These observations showed that CIC-3^{-/-} mice gained more body weight than CIC-3^{+/+} mice in the same feeding condition, suggesting that the normal diet may be efficiently converted for development and growth in CIC-3^{-/-} mice.

3.2 The deletion of CIC-3 partially impaired glucose tolerance in mice consuming a normal diet

The aforementioned details indicated that CIC-3^{-/-} mice could efficiently obtain the needs in a normal diet to gain weight, for which the utilization of lipids and glucose is essential. Thus, the blood lipid and glucose tolerance tests were performed in 12-week-old mice with a normal diet.

As shown in Figure 2A, TG, TC, HDL, and LDL in fasting CIC-3^{-/-} mice were 1.15 ± 0.18 , 2.27 ± 0.16 , 1.93 ± 0.15 , and 0.2 ± 0.02 mM, respectively, which were slightly lower than those in CIC-3^{+/+} mice, but not significant ($n = 7$, $p > 0.05$). Fasting blood glucose (FBG) in CIC-3^{+/+} and CIC-3^{-/-} mice was 5.18 ± 0.28 and 3.97 ± 0.33 mM, respectively ($n = 7-8$, $p < 0.05$). After being intraperitoneally injected with D-glucose doses of 2 g/kg body weight, blood glucose in wide-type mice quickly increased to the peak value of 14.98 ± 0.66 mM at 15 min and then decreased to 6.48 ± 0.37 mM at 120 min; for CIC-3^{-/-} mice, blood glucose increased to 14.33 ± 0.83 mM at 15 min, reached the peak value of 15.53 ± 0.95 mM at 30 min, and then, rapidly decreased to 5.2 ± 0.13 at 120 min (Figure 2B, vs. values in CIC-3^{+/+} mice at the same time, $p < 0.05$). Blood glucose values were normalized according to

the autologous FBG to eliminate the FBG difference between CIC-3^{+/+} and CIC-3^{-/-} mice. As illustrated in Figure 2C, after the intraperitoneal injection of D-glucose for 15 min, the increased folds of blood glucose in CIC-3^{+/+} and CIC-3^{-/-} mice were 2.93 ± 0.18 and 3.69 ± 0.23 , respectively ($p < 0.05$); for 30 min, the blood glucose-increased folds in CIC-3^{+/+} and CIC-3^{-/-} mice were 2.4 ± 0.15 and 4.0 ± 0.29 , respectively ($p < 0.001$); for 90 and 120 min, there were no differences of blood glucose-increased folds between CIC-3^{+/+} and CIC-3^{-/-} mice ($p > 0.05$).

The response to blood glucose increasing for CIC-3^{-/-} mice was torpid, but the efficiency of lowering blood glucose was much higher once started. It is suggested that the deletion of CIC-3 partially impaired glucose tolerance in mice with normal dietary intake.

3.3 The deletion of CIC-3 significantly affected the transcriptional expression of genes in glucolipid metabolism-related pathways

The liver, as one of the major organs, is responsible for glycolipid metabolism (Bechmann et al., 2012; Ye et al., 2017), which is crucial for development and growth. Thus, the transcriptomes of the liver in 3-week-old CIC-3^{+/+} and CIC-3^{-/-} mice were sequenced to investigate the roles of CIC-3 in the glucose metabolism of mice with a normal diet.

Compared to 3-week-old CIC-3^{+/+} mice, 874 DEGs in CIC-3^{-/-} mice were identified, including 589 upregulated genes and 285 downregulated genes (Figure 3A, $n = 4-5$, $p < 0.05$). Among them, Pik3r1 was marked as a positive control gene, which was reported by another study (Jingxuan et al., 2022). Then, all DEGs were analyzed by the enrichment of KEGG pathways. As illustrated in Figure 3B; Supplementary Table S1, the glucose and lipid metabolism-related pathways were significantly clustered ($p < 0.05$), including steroid hormone biosynthesis, the PI3K-Akt signaling pathway, and the regulation of lipolysis

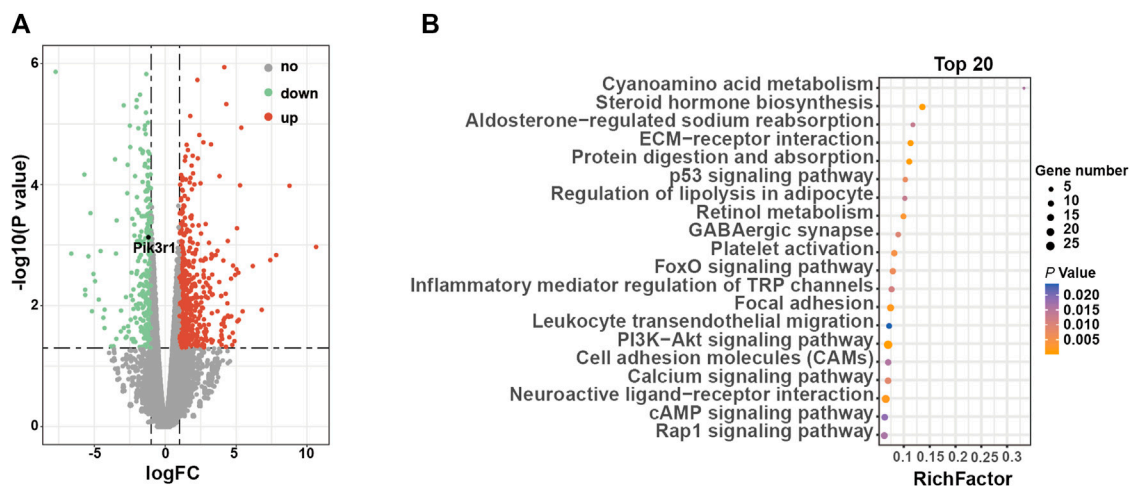


FIGURE 3

CIC-3 deletion significantly changed the transcriptional expression of glucose metabolism-related genes in unweaned mice. (A) Volcano plot of differentially expressed genes in the livers between 3-week-old CIC-3^{+/+} and CIC-3^{-/-} mice (CIC-3^{-/-} v. s. CIC-3^{+/+} mice, $n = 4-5$). (B) Top 20 KEGG enrichment pathways of DEGs.

in adipocytes. Moreover, the enriched pathways of amino acid metabolism were ranked in the top 20 ($p < 0.05$).

The aforementioned details suggested that CIC-3-deletion-caused impairment of glucose tolerance may result from the transcriptional changes of glucose metabolism-related genes.

3.4 The deletion of CIC-3 changed the levels of DNA methylation in CIC-3^{-/-} mice liver

CIC-3 proteins were expressed in the nucleus (Wang et al., 2000; Mao et al., 2012; Zhang et al., 2013a; Liang et al., 2014) and influenced gene expression (Zhang et al., 2013b). However, the roles of nuclear CIC-3 were not elucidated until now. The aforementioned details showed that hundreds of genes were up- or downregulated by CIC-3 deletion, suggesting that the regulation of gene expression was one of the roles of CIC-3 proteins in the nucleus. DNA methylation is the heritable and reversible controller of gene expression. Then, we observed the effects of DNA methylation on glucose metabolism-related genes in CIC-3^{-/-} mice livers.

The levels of DNA methylation in the 3-week-old mice livers were analyzed by RRBS. As illustrated in Figure 4A, over 98% of methylated cytosines occurred in a CG context, and nearly 2% of methylated cytosines were detected in CHH and CHG contexts. Then, the methylated cytosine sites in the CG context were further explored. Between CIC-3^{+/+} and CIC-3^{-/-} mice of CG contexts, methylated cytosine sites in the transcription start site's upstream 2000 bp, gene-body, and the transcription termination site's downstream 2000 bp were different, but they were not different in the CpG islands (Figure 4B). Additionally, a total of 2,540 differentially methylated regions were found; compared to CIC-3^{+/+} mice, there were 1,347 upregulated DMRs and 1,193 downregulated DMRs in CIC-3^{-/-} mice (Figure 4C); 78.18% of DMRs were overlapped in the gene-body region,

and 18.89% of DMRs were located in the promoter of genes (Figure 4D). The genes targeted by DMRs in the CG context were enriched by the analysis of KEGG pathways, the top 25 pathways of which are presented in Figure 4E. The glucose metabolism-associated pathways were significantly enriched, such as type II diabetes mellitus, insulin resistance, metabolic pathways, and citrate cycle. Additionally, the DMR-targeted genes, such as Nos3, Pik3r1, Socs1, and Acly, were identified and involved in these pathways.

These indicated that CIC-3 deletion could change the DNA methylation levels of genes related to glucose metabolism in unweaned mice.

3.5 CIC-3 was involved in the glucose metabolism-related gene expression via DNA methylation

DNA methylation is an important pattern to regulate gene expression, but the levels of gene expression are not always in correspondence with the levels of methylation. Then, the relationships between DMR-anchored genes and DEGs were further explored.

As shown in Figure 5A, there were 92 overlapped genes between DMR-anchored genes and DEGs. These genes were enriched by the analysis of KEGG pathways, the glucose metabolism-related pathways of which were listed in the top 20, such as type II diabetes mellitus, insulin resistance, and metabolic pathways (Figure 5B, $p < 0.05$). The correlations of overlapped genes between gene expression and DNA methylation were analyzed. There were 14 genes whose expressions were negatively correlated with the methylation levels in gene-body ($p < 0.05$); the expression of five genes was positively correlated with the methylation levels in the gene-body ($p < 0.05$); Onecut1 was the only gene whose expression was positively

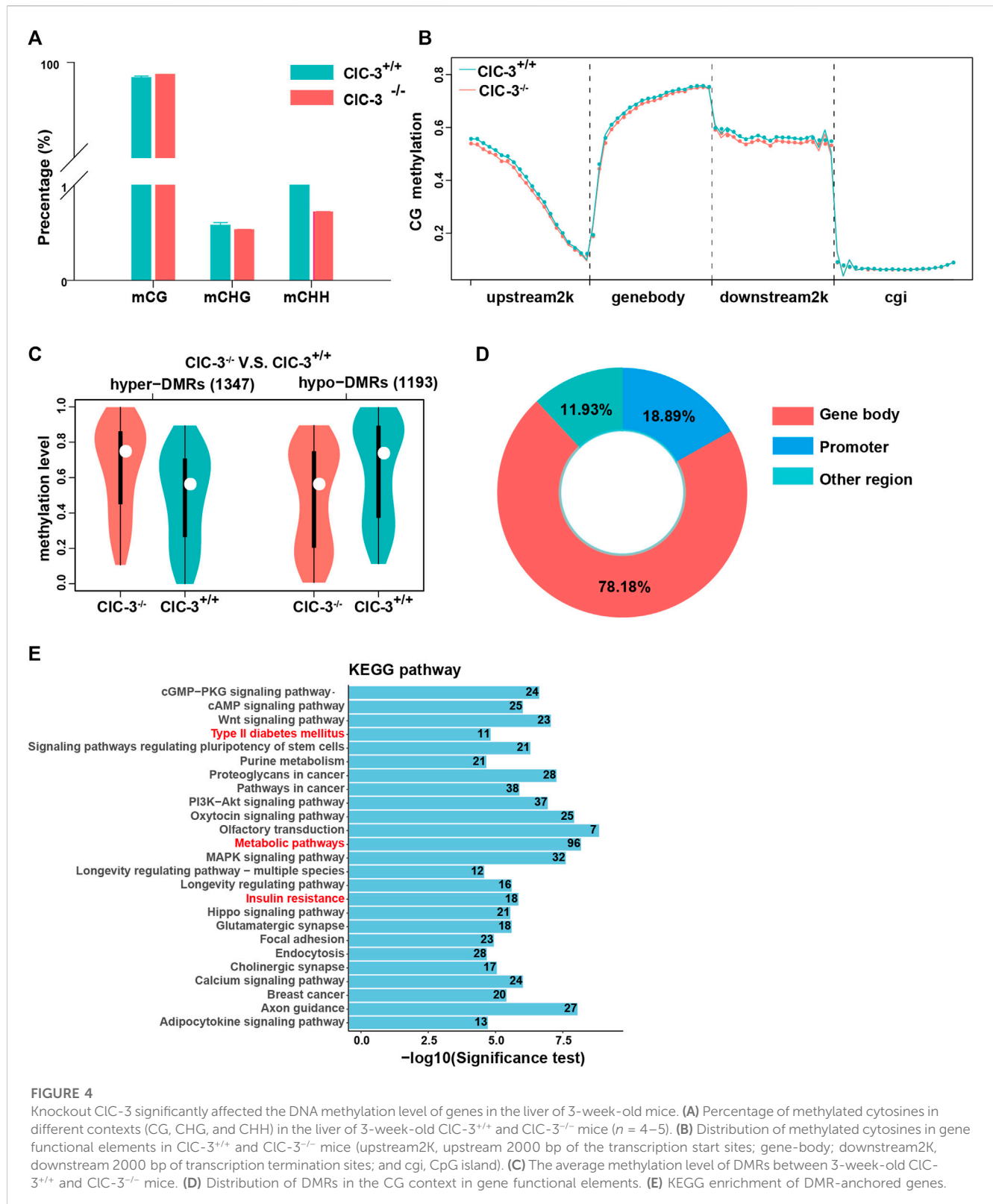


FIGURE 4

Knockout CIC-3 significantly affected the DNA methylation level of genes in the liver of 3-week-old mice. (A) Percentage of methylated cytosines in different contexts (CG, CHG, and CHH) in the liver of 3-week-old CIC-3^{+/+} and CIC-3^{-/-} mice (n = 4–5). (B) Distribution of methylated cytosines in gene functional elements in CIC-3^{+/+} and CIC-3^{-/-} mice (upstream2K, upstream 2000 bp of the transcription start sites; gene-body; downstream2K, downstream 2000 bp of transcription termination sites; and cgi, CpG island). (C) The average methylation level of DMRs between 3-week-old CIC-3^{+/+} and CIC-3^{-/-} mice. (D) Distribution of DMRs in the CG context in gene functional elements. (E) KEGG enrichment of DMR-anchored genes.

correlated with the methylation levels in the gene-body's upstream 2K regions ($p < 0.05$, [Supplementary Table S2](#)). These indicated that CIC-3 deletion affected the expressions of specific genes, which were closely associated with DNA methylation in unweaned mice.

Nos3, Pik3r1, Socs1, and Acl1, as the overlapped genes, were enriched in the glucose metabolism-associated pathways. Both Socs1 and Pik3r1 were enriched in the PI3K-Akt and insulin signaling pathways. In the unweaned CIC-3^{-/-} mice, the transcriptional levels of Socs1 and Pik3r1 were, respectively,

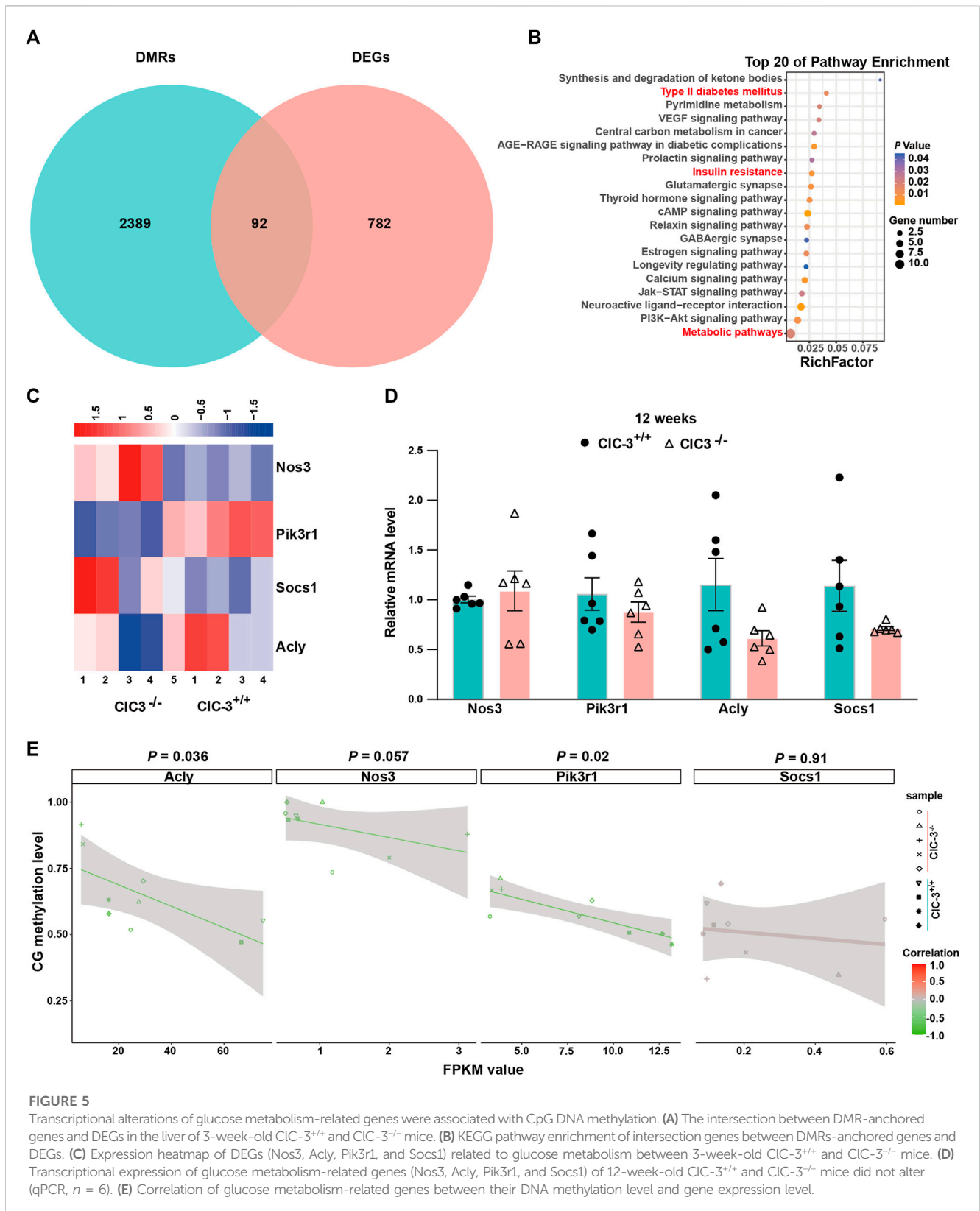


FIGURE 5

Transcriptional alterations of glucose metabolism-related genes were associated with CpG DNA methylation. (A) The intersection between DMR-anchored genes and DEGs in the liver of 3-week-old CIC-3^{+/+} and CIC-3^{-/-} mice. (B) KEGG pathway enrichment of intersection genes between DMRs-anchored genes and DEGs. (C) Expression heatmap of DEGs (Nos3, Acly, Pik3r1, and Socs1) related to glucose metabolism between 3-week-old CIC-3^{+/+} and CIC-3^{-/-} mice. (D) Transcriptional expression of glucose metabolism-related genes (Nos3, Acly, Pik3r1, and Socs1) of 12-week-old CIC-3^{+/+} and CIC-3^{-/-} mice did not alter (qPCR, n = 6). (E) Correlation of glucose metabolism-related genes between their DNA methylation level and gene expression level.

upregulated and downregulated ($p < 0.05$), which could inhibit the insulin receptor-mediated glycogen synthesis. Acly and Nos3 were enriched in the citrate cycle, insulin resistance, and PI3K-Akt signaling pathways. In the unweaned CIC-3^{-/-} mice, the

transcriptional level of Nos3 was upregulated ($p < 0.05$), which could block the transduction of insulin receptor signaling; Acly was downregulated ($p < 0.05$), which inhibited the breakdown of citric acid to decrease lipid synthesis and increase energy supply

(Figure 5C). Additionally, the expressions of *Nos3*, *Pik3r1*, *Socs1*, and *Acly* were assayed in adult mice with normal dietary consumption; as illustrated in Figure 5D, there were no differences in these four genes' expressions between *CIC-3^{+/+}* and *CIC-3^{-/-}* mice ($n = 6$, $p > 0.05$).

Furthermore, the Pearson correlations between these genes' expressions and their DNA methylation levels were calculated. As illustrated in Figure 5E, the FPKM values of *Pik3r1* and *Acly* were negatively correlated with their DNA methylation levels, and the Pearson values for *Pik3r1* and *Acly* were -0.75 and -0.7 , respectively ($n = 4-5$, $p < 0.05$); the Pearson values for *Nos3* and *Socs1* were -0.65 and 0.04 , respectively ($n = 4-5$, $p > 0.05$). These suggested that DNA methylation was one of the ways for *CIC-3* to regulate the expressions of glucose metabolism-associated genes.

4 Discussion

The development of metabolic disease is a complex progress involving multiple factors, such as diet (Zinöcker and Lindseth, 2018), genetics (Barroso and McCarthy, 2019), gut microbiome (Turnbaugh et al., 2006; Marchesi et al., 2016), and age (Lee and Park, 2020). Glucose metabolism is the central reaction of all biological metabolic processes, and its dysfunction will lead to the emergence of obesity, diabetes, and cardiovascular diseases. Thus, it is crucial to rebalance glucose metabolism for the control of metabolic diseases.

In addition to participating in proliferation, migration, apoptosis, and drug transport (Zhang et al., 2006; Cuddapah et al., 2012; Zhang et al., 2013b; Ganapathi et al., 2013; Zhou et al., 2018; Chen et al., 2019; Feng et al., 2021), *CIC-3* was verified to actively regulate the glycolipid metabolism. *CIC-3* deletion would improve the phenotypes of dysglycemic metabolism and the impairment of insulin sensitivity in mice with an abnormal diet (Deriy et al., 2009; Li et al., 2009; Huang et al., 2014; Ma et al., 2019). These improvements were the comprehensive results of the changes in numerous genes' expressions affected by *CIC-3* deletion.

Gene expression is always the result of gene-environmental interaction, of which DNA methylation, histone modification, and noncoding RNAs are key mediators. A small quantity of *CIC-3* proteins localized in the nucleus (Wang et al., 2000; Mao et al., 2012; Zhang et al., 2013a; Liang et al., 2014) would provide a possible manner to participate in the gene expression. However, there was no idea about the effects of *CIC-3* deletion on the changes in DNA methylation in mice with a normal diet.

We previously reported that the unweaned *CIC-3^{-/-}* mice had lower body weights and smaller parenchymal organs (Jing et al., 2022). The present study showed that 4-, 6-, and 8-week-old *CIC-3^{-/-}* mice with *ad libitum* self-feeding normal diet had lower body weights than the same aged *CIC-3^{+/+}* mice, which is consistent with another report (Dickerson et al., 2002). *CIC-3^{-/-}* mice aged 10 and 12 weeks had similar body weights to the wild-type mice, but the heart, liver, and brain weights in 12-week-old *CIC-3^{-/-}* mice were still lower (Figure 1). Disruption of *CIC-3* leads to a loss of the hippocampus in 7-month-old mice (Stobrawa et al., 2001). This was not evidenced in mice younger than 7 months,

but *CIC-3* deletion slowed the brain growth of adult mice, not the unweaned mice (Jing et al., 2022). These indicated that the inhibition of growth and organ development by *CIC-3* deletion may not be invariable along with the increase of age in *CIC-3^{-/-}* mice with a normal diet.

Glycolipid metabolism is vitally important for growth and organ development. In contrast with that of *CIC-3^{-/-}* mice consuming a high-fat diet (Ma et al., 2019), there were no significant differences in blood lipids between *CIC-3^{-/-}* and *CIC-3^{+/+}* mice with a normal diet at the age of 12 weeks; intraperitoneal glucose tolerance test demonstrated that *CIC-3* deletion delayed the response to blood glucose increasing and enhanced the efficiency of lowering blood glucose once started (Figure 2). *CIC-3^{-/-}* mice had a partial impairment of glucose tolerance in the condition of *ad libitum* self-feeding normal diet, which may be associated with the inhibition of insulin secretion by *CIC-3* knocking out (Barg et al., 2001; Deriy et al., 2009; Li et al., 2009; Niu et al., 2021). This finding appeared to be inconsistent with the improvement of glucose tolerance impairment in *CIC-3^{-/-}* mice with obesity or diabetes (Huang et al., 2014; Ma et al., 2019). Of course, the dietary difference among these mice was an inevitable factor that must be considered, which would have a profound impact on the expression of metabolic genes.

One of the most important organs for regulating glycolipid metabolism is the liver (Bechmann et al., 2012; Ye et al., 2017). Our previous and present studies showed that the livers in the unweaned (Jing et al., 2022) and normal diet-consuming *CIC-3^{-/-}* mice were all smaller. The liver may be one of the determinants contributing to the *CIC-3^{+/+}* mice phenotypes, especially glucose metabolism in the condition of normal diet intake, whose underlying mechanisms would be explored by the transcriptomic and epigenetic alterations. *CIC-3* deletion caused the transcribed changes of 874 genes, a part of which was enriched in the glucose and lipid metabolism-related pathways, including steroid hormone biosynthesis, the PI3K-Akt signaling pathway, and regulation of lipolysis in adipocyte (Figure 3); 2540 DMR-anchored genes were partially clustered in the glucose metabolism-associated pathways, such as type II diabetes mellitus, insulin resistance, metabolic pathways, and citrate cycle (Figure 4). It is implied that the *CIC-3* deletion-associated genes in the control of methylation were vital actors in regulating glucose metabolism.

The intersected genes between DEG- and DMR-targeted genes were gathered in type II diabetes mellitus, insulin resistance, and metabolic pathways, which referred to *Nos3*, *Pik3r1*, *Socs1*, and *Acly* (Figure 5). The upregulated *Nos3*, *Socs1*, and downregulated *Pik3r1* inhibited the transduction of insulin receptor signaling, being associated with insulin resistance; the downregulated *Acly* inhibited the breakdown of citric acid, increasing energy production (Zhang et al., 2014; Piñeros Alvarez et al., 2017; Kempinska-Podhorodecka et al., 2019). There were only *Pik3r1* and *Acly*, whose transcription levels were closely related to DNA methylation levels, implying that the methylated modification was not the only way for *CIC-3* to participate in the gene expression. However, the specific expressions of these genes were crucial factors to bring out a petite unweaned *CIC-3^{-/-}* mouse. Interestingly, it is faster to gain body weight for adult *CIC-3^{-/-}* mice consuming a normal diet. The answers may be found from the unexpected results that there were no differences in *Nos3*, *Pik3r1*,

Socs1, and Acly transcriptional levels between *ClC-3^{-/-}* and *ClC-3^{+/+}* mice. It suggested that diet types could drive the change of gene expression again in *ClC-3*-deficient mice.

In conclusion, *ClC-3* was involved in glucose metabolism and associated with the methylated modification to regulate the transcriptions of glucose metabolism-related genes, whose expressions could be driven to change again by a personalized diet-style intervention. Therefore, we proposed that *ClC-3* could be a potential target to rebalance the dysfunction of glucose or lipid metabolism caused by an unhealthy diet.

Data availability statement

The data presented in the study are deposited in the NCBI repository, accession numbers are PRJNA956595 and PRJNA956309.

Ethics statement

The animal study was reviewed and approved by the Laboratory Animal Administration Committee of Xi'an Jiaotong University.

Author contributions

Conceptualization: HZ and LF; methodology: HZ, LF, and ZJ; investigation: ZJ, YW, SC, YR, RL, SD, and WZ; writing—original draft preparation: ZJ, YW, and HZ; writing—review and editing: HZ and ZJ; supervision: HZ and LF; and funding acquisition: HZ and LF. All authors contributed to the article and approved the submitted version.

Funding

This work was supported by the National Natural Science Foundation of China (81402312 to HZ; 62176208 to LF), the

References

- Aslibekyan, S., Demerath, E. W., Mendelson, M., Zhi, D., Guan, W., Liang, L., et al. (2015). Epigenome-wide study identifies novel methylation loci associated with body mass index and waist circumference. *Obes. (Silver Spring)* 23, 1493–1501. doi:10.1002/oby.21111
- Barg, S., Huang, P., Eliasson, L., Nelson, D. J., Obermüller, S., Rorsman, P., et al. (2001). Priming of insulin granules for exocytosis by granular Cl(-) uptake and acidification. *J. Cell Sci.* 114, 2145–2154. doi:10.1242/jcs.114.11.2145
- Barroso, I., and McCarthy, M. I. (2019). The genetic basis of metabolic disease. *Cell* 177, 146–161. doi:10.1016/j.cell.2019.02.024
- Bechmann, L. P., Hannivoort, R. A., Gerken, G., Hotamisligil, G. S., Trauner, M., and Canbay, A. (2012). The interaction of hepatic lipid and glucose metabolism in liver diseases. *J. Hepatol.* 56, 952–964. doi:10.1016/j.jhep.2011.08.025
- Chen, Q., Liu, X., Luo, Z., Wang, S., Lin, J., Xie, Z., et al. (2019). Chloride channel-3 mediates multidrug resistance of cancer by upregulating P-glycoprotein expression. *J. Cell Physiol.* 234, 6611–6623. doi:10.1002/jcp.27402
- Cuddapah, V. A., Habela, C. W., Watkins, S., Moore, L. S., Barclay, T. T., and Sontheimer, H. (2012). Kinase activation of *ClC-3* accelerates cytoplasmic condensation during mitotic cell rounding. *Am. J. Physiol. Cell Physiol.* 302, C527–C538. doi:10.1152/ajpcell.00248.2011
- Deriy, L. V., Gomez, E. A., Jacobson, D. A., Wang, X., Hopson, J. A., Liu, X. Y., et al. (2009). The granular chloride channel *ClC-3* is permissive for insulin secretion. *Cell Metab.* 10, 316–323. doi:10.1016/j.cmet.2009.08.012
- Dickerson, L. W., Bonthius, D. J., Schutte, B. C., Yang, B., Barna, T. J., Bailey, M. C., et al. (2002). Altered GABAergic function accompanies hippocampal degeneration in mice lacking *ClC-3* voltage-gated chloride channels. *Brain Res.* 958, 227–250. doi:10.1016/s0006-8993(02)03519-9
- Du, Y. H., and Guan, Y. Y. (2015). Chloride channels - new targets for the prevention of stroke. *Curr. Vasc. Pharmacol.* 13, 441–448. doi:10.2174/1570161112666141014145040
- Duan, D. D. (2011). The *ClC-3* chloride channels in cardiovascular disease. *Acta Pharmacol. Sin.* 32, 675–684. doi:10.1038/aps.2011.30
- Feng, J., Peng, Z., Gao, L., Yang, X., Sun, Z., Hou, X., et al. (2021). *ClC-3* promotes paclitaxel resistance via modulating tubulins polymerization in ovarian cancer cells. *Biomed. Pharmacother.* 138, 111407. doi:10.1016/j.biopha.2021.111407
- Ganapathi, S. B., Wei, S. G., Zaremba, A., Lamb, F. S., and Shears, S. B. (2013). Functional regulation of *ClC-3* in the migration of vascular smooth muscle cells. *Hypertension* 61, 174–179. doi:10.1161/hypertensionaha.112.194209
- Hu, C., Peng, K., Wu, Q., Wang, Y., Fan, X., Zhang, D. M., et al. (2021). HDAC1 and 2 regulate endothelial VCAM-1 expression and atherogenesis by suppressing methylation of the *GATA6* promoter. *Theranostics* 11, 5605–5619. doi:10.7150/thno.55878
- Huang, Y. Y., Huang, X. Q., Zhao, L. Y., Sun, F. Y., Chen, W. L., Du, J. Y., et al. (2014). *ClC-3* deficiency protects preadipocytes against apoptosis induced by palmitate *in vitro* and in type 2 diabetes mice. *Apoptosis* 19, 1559–1570. doi:10.1007/s10495-014-1021-0

Natural Science Basic Research Project of Shannxi Province (2022JM-515 to HZ), and Guangzhou Huayin Health Medical Group Co., Ltd. (20201065-ZKT05 to HZ).

Acknowledgments

The authors thank Deng Zhiqin from the First Affiliated Hospital of Shen Zhen University for providing *ClC-3*-modified heterozygous mice.

Conflict of interest

YW was employed by Guangzhou Huayin Medical Laboratory Center Ltd.

The remaining authors declare that the research was conducted in the absence of any commercial or financial relationships that could be construed as a potential conflict of interest.

The handling editor, YL, declared a shared affiliation with the authors ZJ, HZ, SC, YR, RL, SD, WZ, and LF at the time of review.

Publisher's note

All claims expressed in this article are solely those of the authors and do not necessarily represent those of their affiliated organizations, or those of the publisher, the editors, and the reviewers. Any product that may be evaluated in this article, or claim that may be made by its manufacturer, is not guaranteed or endorsed by the publisher.

Supplementary material

The Supplementary Material for this article can be found online at: <https://www.frontiersin.org/articles/10.3389/fcell.2023.1196684/full#supplementary-material>

- Jin, Z., Cheng, Y., Gu, W., Zheng, Y., Sato, F., Mori, Y., et al. (2009). A multicenter, double-blinded validation study of methylation biomarkers for progression prediction in Barrett's esophagus. *Cancer Res.* 69, 4112–4115. doi:10.1158/0008-5472.Can-09-0028
- Jing, Z., Li, C., Liu, R., Ren, Y., Cui, S., Zhao, W., et al. (2022). Effect of Clcn3 knockout on parenchymal organs in young mice. *Acta Lab. Anim. Sci. Sin.* 30, 1532–1543.
- Jingxuan, L., Litian, M., Yanyang, T., and Jianfang, F. (2022). Knockdown of CLC-3 may improve cognitive impairment caused by diabetic encephalopathy. *Diabetes Res. Clin. Pract.* 190, 109970. doi:10.1016/j.diabres.2022.109970
- Kempinska-Podhorodecka, A., Wunsch, E., Milkiewicz, P., Stachowska, E., and Milkiewicz, M. (2019). The association between SOCS1-1656g>A polymorphism, insulin resistance and obesity in nonalcoholic fatty liver disease (NAFLD) patients. *J. Clin. Med.* 8, 1912. doi:10.3390/jcm8111912
- Lee, H. S., and Park, T. (2020). The influences of DNA methylation and epigenetic clocks, on metabolic disease, in middle-aged Koreans. *Clin. Epigenetics* 12, 148. doi:10.1186/s13148-020-00936-z
- Li, D. Q., Jing, X., Salehi, A., Collins, S. C., Hoppa, M. B., Rosengren, A. H., et al. (2009). Suppression of sulfonylurea- and glucose-induced insulin secretion *in vitro* and *in vivo* in mice lacking the chloride transport protein CLC-3. *Cell Metab.* 10, 309–315. doi:10.1016/j.cmet.2009.08.011
- Liang, W., Huang, L., Zhao, D., He, J. Z., Sharma, P., Liu, J., et al. (2014). Swelling-activated Cl⁻ currents and intracellular CLC-3 are involved in proliferation of human pulmonary artery smooth muscle cells. *J. Hypertens.* 32, 318–330. doi:10.1097/hjh.000000000000013
- Ma, M. M., Jin, C. C., Huang, X. L., Sun, L., Zhou, H., Wen, X. J., et al. (2019). Clcn3 deficiency ameliorates high-fat diet-induced obesity and adipose tissue macrophage inflammation in mice. *Acta Pharmacol. Sin.* 40, 1532–1543. doi:10.1038/s41401-019-0229-5
- Mao, J., Li, X., Chen, W., Xu, B., Zhang, H., Li, H., et al. (2012). Cell cycle-dependent subcellular distribution of CLC-3 in HeLa cells. *Histochem Cell Biol.* 137, 763–776. doi:10.1007/s00418-012-0937-0
- Marchesi, J. R., Adams, D. H., Fava, F., Hermes, G. D., Hirschfield, G. M., Hold, G., et al. (2016). The gut microbiota and host health: A new clinical frontier. *Gut* 65, 330–339. doi:10.1136/gutjnl-2015-309990
- Niu, D., Li, L., and Xie, Z. (2021). CLC-3: A novel promising therapeutic target for atherosclerosis. *J. Cardiovasc. Pharmacol. Ther.* 26, 550–561. doi:10.1177/10742484211023639
- Payne, S. R. (2010). From discovery to the clinic: The novel DNA methylation biomarker (m)SEPT9 for the detection of colorectal cancer in blood. *Epigenomics* 2, 575–585. doi:10.2217/epi.10.35
- Piñeros Alvarez, A. R., Glosion-Byers, N., Brandt, S., Wang, S., Wong, H., Sturgeon, S., et al. (2017). SOCS1 is a negative regulator of metabolic reprogramming during sepsis. *JCI Insight* 2, e92530. doi:10.1172/jci.insight.92530
- Qin, X., Karlsson, I. K., Wang, Y., Li, X., Pedersen, N., Reynolds, C. A., et al. (2021). The epigenetic etiology of cardiovascular disease in a longitudinal Swedish twin study. *Clin. Epigenetics* 13, 129. doi:10.1186/s13148-021-01113-6
- Shao, Y., Shaw, M., Todd, K., Khrestian, M., D'Aleo, G., Barnard, P. J., et al. (2018). DNA methylation of TOMM40-APOE-APOC2 in Alzheimer's disease. *J. Hum. Genet.* 63, 459–471. doi:10.1038/s10038-017-0393-8
- Stobrawa, S. M., Breiderhoff, T., Takamori, S., Engel, D., Schweizer, M., Zdebik, A. A., et al. (2001). Disruption of CLC-3, a chloride channel expressed on synaptic vesicles, leads to a loss of the hippocampus. *Neuron* 29, 185–196. doi:10.1016/s0896-6273(01)00189-1
- Sun, H., Saeedi, P., Karuranga, S., Pinkepank, M., Ogurtsova, K., Duncan, B. B., et al. (2022). IDF Diabetes Atlas: Global, regional and country-level diabetes prevalence estimates for 2021 and projections for 2045. *Diabetes Res. Clin. Pract.* 183, 109119. doi:10.1016/j.diabres.2021.109119
- Teschendorff, A. E., Menon, U., Gentry-Maharaj, A., Ramus, S. J., Weisenberger, D. J., Shen, H., et al. (2010). Age-dependent DNA methylation of genes that are suppressed in stem cells is a hallmark of cancer. *Genome Res.* 20, 440–446. doi:10.1101/gr.103606.109
- Toperoff, G., Aran, D., Kark, J. D., Rosenberg, M., Dubnikov, T., Nissan, B., et al. (2012). Genome-wide survey reveals predisposing diabetes type 2-related DNA methylation variations in human peripheral blood. *Hum. Mol. Genet.* 21, 371–383. doi:10.1093/hmg/ddr472
- Turnbaugh, P. J., Ley, R. E., Mahowald, M. A., Magrini, V., Mardis, E. R., and Gordon, J. I. (2006). An obesity-associated gut microbiome with increased capacity for energy harvest. *Nature* 444, 1027–1031. doi:10.1038/nature05414
- Wang, L., Chen, L., and Jacob, T. J. (2000). The role of CLC-3 in volume-activated chloride currents and volume regulation in bovine epithelial cells demonstrated by antisense inhibition. *J. Physiol.* 524 (1), 63–75. doi:10.1111/j.1469-7793.2000.t01-1-00063.x
- Xu, X., Su, S., Barnes, V. A., De Miguel, C., Pollock, J., Ownby, D., et al. (2013). A genome-wide methylation study on obesity: Differential variability and differential methylation. *Epigenetics* 8, 522–533. doi:10.4161/epi.24506
- Yang, B. T., Dayeh, T. A., Volkov, P. A., Kirkpatrick, C. L., Malmgren, S., Jing, X., et al. (2012). Increased DNA methylation and decreased expression of PDX-1 in pancreatic islets from patients with type 2 diabetes. *Mol. Endocrinol.* 26, 1203–1212. doi:10.1210/me.2012-1004
- Ye, D. W., Rong, X. L., Xu, A. M., and Guo, J. (2017). Liver-adipose tissue crosstalk: A key player in the pathogenesis of glucolipid metabolic disease. *Chin. J. Integr. Med.* 23, 410–414. doi:10.1007/s11655-017-2810-4
- Zhang, H., Li, H., Yang, L., Deng, Z., Luo, H., Ye, D., et al. (2013a). The CLC-3 chloride channel associated with microtubules is a target of paclitaxel in its induced-apoptosis. *Sci. Rep.* 3, 2615. doi:10.1038/srep02615
- Zhang, H. N., Zhou, J. G., Qiu, Q. Y., Ren, J. L., and Guan, Y. Y. (2006). CLC-3 chloride channel prevents apoptosis induced by thapsigargin in PC12 cells. *Apoptosis* 11, 327–336. doi:10.1007/s10495-006-3980-2
- Zhang, H., Zhang, L., Chen, H., Chen, Y. Q., Chen, W., Song, Y., et al. (2014). Enhanced lipid accumulation in the yeast *Yarrowia lipolytica* by over-expression of ATP:citrate lyase from *Mus musculus*. *J. Biotechnol.* 192, 78–84. doi:10.1016/j.jbiotec.2014.10.004
- Zhang, H., Zhu, L., Zuo, W., Luo, H., Mao, J., Ye, D., et al. (2013b). The CLC-3 chloride channel protein is a downstream target of cyclin D1 in nasopharyngeal carcinoma cells. *Int. J. Biochem. Cell Biol.* 45, 672–683. doi:10.1016/j.biocel.2012.12.015
- Zhou, F. M., Huang, Y. Y., Tian, T., Li, X. Y., and Tang, Y. B. (2018). Knockdown of chloride channel-3 inhibits breast cancer growth *in vitro* and *in vivo*. *J. Breast Cancer* 21, 103–111. doi:10.4048/jbc.2018.21.2.103
- Zinöcker, M. K., and Lindseth, I. A. (2018). The western diet-microbiome-host interaction and its role in metabolic disease. *Nutrients* 10, 365. doi:10.3390/nu10030365